Hot Pixels Suppression in Structured Illumination Microscopy

Jakub POSPÍŠIL

Dept. of Radioelectronics, Faculty of Electrical Engineering, Czech Technical University in Prague, Technická 2, 166 27 Praha, Czech Republic

E-mail: pospij27@fel.cvut.cz

Abstract. *Structured Illumination Microscopy (SIM) is a super-resolution fluorescence technique which enables to enhance the resolution of optical microscopes beyond the diffraction limit. The final super-resolution image quality strongly depends on the performance of SIM image reconstruction. Standard SIM methods require the input images with high signal to noise ratio (SNR). However, the light emitted from the sample labeled with a fluorescence dye is weak. Therefore, the long exposure time (in the order of seconds) is required. The low number of photons, due to the weakness of fluorescence dye, captured by camera sensor causes the high bias of the acquired image by additional noise sources (read-out noise, Poisson noise). Further, the long exposure time leads to the thermal noise. In this paper, we focus on the thermal noise, especially on the hot pixels, whose values are four or more standard deviations above the mean. These hot pixels dramatically decrease the dynamic range of final discrete value image. Therefore, the SIM image reconstruction may fail because of the normalization and rounding during the reconstruction.*

Keywords

Super-resolution, structured illumination microscopy, hot pixel, reconstruction.

1. Introduction

Light microscopy is widely used in molecular and cell biology. Fluorescence microscopy allows one to investigate live cell dynamics with high specificity. Despite this advantage, standard fluorescence microscopes are not able to visualize specimen structures smaller than the Abbe diffraction limit [1]. Super-resolution microscopy techniques increase the resolution of optical microscopes beyond the diffraction limit. These approaches include stochastic optical reconstruction microscopy [2] (STORM), super-resolution optical fluctuation imaging [3], [4] (SOFI), photoactivated localization microscopy [5] (PALM), stimulated emission depletion microscopy [6] (STED) and structured illumination microscopy [1], [7], [8] (SIM). This paper is focused on the input raw images preprocessing for SIM reconstruction. Especially on the hot pixel detection and suppression, which is essential for the future SIM applications in cell biology. Several methods correcting the appearance of hot pixels are now available [9]–[12]. However, these methods require special equipment or they have high computational demand.

2. Structured Illumination Microscopy

SIM is a super-resolution microscopy technique which uses harmonic illumination patterns to copy high information content on lower frequencies where it can be recovered using multiple illumination patterned images and complex reconstruction methods. A fluorescently labeled sample is illuminated by harmonic pattern with the spatial frequency close to the maximum (cut-off) frequency supported by optical transfer function (OTF). The high frequency (HR) information is encoded into observed image through aliasing (Fig. 1a). Fourier transform of observed image can be mathematically described as

$$\begin{aligned}\widetilde{D}_n(\boldsymbol{k}) &= \left[\tilde{S}(\boldsymbol{k}) \otimes \tilde{I}_n(\boldsymbol{k})\right] \cdot \widetilde{H}(\boldsymbol{k}) \\ &= \frac{I_0}{2}[\tilde{S}(\boldsymbol{k}) - \frac{m}{2}\tilde{S}(\boldsymbol{k}-\boldsymbol{p}_\theta)e^{-j\varphi} \\ &\quad - \frac{m}{2}\tilde{S}(\boldsymbol{k}+\boldsymbol{p}_\theta)e^{+j\varphi}] \cdot \widetilde{H}(\boldsymbol{k}), \end{aligned} \quad (1)$$

where $\tilde{S}(\boldsymbol{k})$ and $\tilde{I}_n(\boldsymbol{k})$ is Fourier transform of specimen and illumination pattern, respectively. The OTF is represented by $\widetilde{H}(\boldsymbol{k})$, and $\otimes$ is convolution operator. I_0 is the peak illumination intensity of pattern with modulation factor m.

Eq. (1) suggests that $\widetilde{D}_n(\boldsymbol{k})$ is a combination of spectral components $\tilde{S}(\boldsymbol{k})$ and $\tilde{S}(\boldsymbol{k} \pm \boldsymbol{p}_\theta)$, where the illumination frequency vector $\boldsymbol{p}_\theta$ is equal to $\boldsymbol{p}_\theta = (p \cdot cos\theta, p \cdot sin\theta)$, θ indicates the pattern orientation and φ is the phase of illumination pattern. If the pattern spatial frequency, orientation and phase shift are known, the shifted spectral components can be separated, shifted to their proper

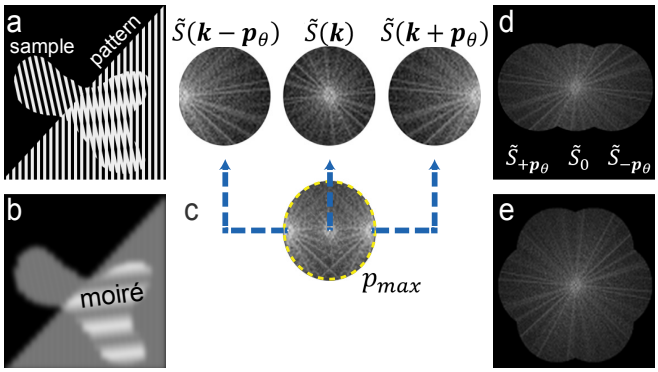

Fig. 1 Principle scheme of SIM reconstruction. (a) Moiré effect due to the overlap of striped sample and illumination pattern. (b) Observed image of illuminated sample passed through the diffraction limited optical system. (c) Example Fourier transform of observed image and its decomposition to three spectral components (p_{max} is cut-off frequency). (d) Alignment of these three spectral components. The final width of Fourier space is increased twice. (e) Example Fourier space increased with three orientations of the illumination pattern.

positions and aligned together (Fig. 1c-d). By acquiring multiple images with phase shifted sinusoidal pattern (usually 3-5), a set of interrelated complex equations is obtained. A high-resolution image is reconstructed by solving this linear system of equations.

3. Acquisition and Samples

The resolution test target designed to measure accuracy and performance of the optical microscopes has been used in our experiment. The images have been acquired by fluorescence microscope described below.

3.1 Microscope setup

Used setup is based on an Olympus IX71 microscope with a UPLASPO 100×/1.40 NA (numerical aperture) oil immersion objective [7], [13] with NEO sCMOS camera with IQ software (Andor). The back-projected pixel size was 42 nm. Focus was adjusted using a piezo-Z stage. A high-speed ferroelectric liquid crystal on silicon (LCOS) microdisplay produced the illumination pattern [7], [13], [14]. The display was illuminated by LED system based on the high-power LED with emission maxima at 525 nm. The light was then filtered with band pass filter (Chroma) and vertically polarized. Final polarized illumination pattern was imaged through the objective into the sample. The microdisplay allows one to create any desired illumination pattern. For our experiments, the illumination masks consisted of the thick lines with a gap between them. Three pattern orientations were used (90°, 45° and 135°).

3.2 Samples

The Argolight test targets are designed for assessing the performances of fluorescence-based microscopy imaging systems. The testing slides are constructed with a special glass piece set on a stainless-steel carrier. Each slide contains a different fluorescence pattern (see Fig. 6 in supplementary), which can be excited with light with wavelength from 300 nm to 550 nm (maximum emission efficiency is at around 340 nm).

Images used in our experiment have been acquired by Andor camera (described above) with exposure time in the range of 200 ms to 3500 ms. Significant increase of hot pixels appears in samples with longer exposure time. The image stack acquired with 2000 ms exposure time is used as a representative image in this text.

4. Noise

All acquired images are contaminated by noise from different sources. These sources include photon noise, read-out noise (amplifier noise, on-chip electronic noise and Johnson–Nyquist noise), thermal noise (dark current and hot pixels) and quantization noise.

4.1 Read-out noise

Read-out noise, or just read noise, is usually stated in terms of the number of electrons introduced per pixel into final signal during acquisition. The charge in each pixel is converted voltage which is amplified before digitization in the analogue to digital converter (A/D). Each amplifier and A/D circuit produces a random additional value which slightly increase or decrease the output. Thus, the reading out the same pixel twice, each time with identical charge, a slightly different response may be produced. This yields to unwanted fluctuation in each pixel in output image [15], [16].

4.2 Dark current (Hot pixels)

Dark current is a stochastic process which yields a Poisson distribution from the number of electrons generated in a fix time interval. Some pixels on the sensor suffer severely from the dark current, and after a few seconds of integration, a dark image looks like an image with stars. This high peaks (also known as hot pixels) dramatically reduce the dynamic range of the final image. Dark current strongly depends on the operating temperature of the camera [16].

5. Noise reduction

There are several methods to eliminate some of the noise sources described in chapter 4. These methods include the proper electrical design of whole camera system, carefully selected conditions during acquisition (e.g. sensor cooling in the range -40°C to -90°C), or the calibration and reduction process. The calibration set of images consists of three basic calibration images: bias, dark field and flat field [15], [17]. In case, these calibration images are not available, the noise has to be estimated from acquired data.

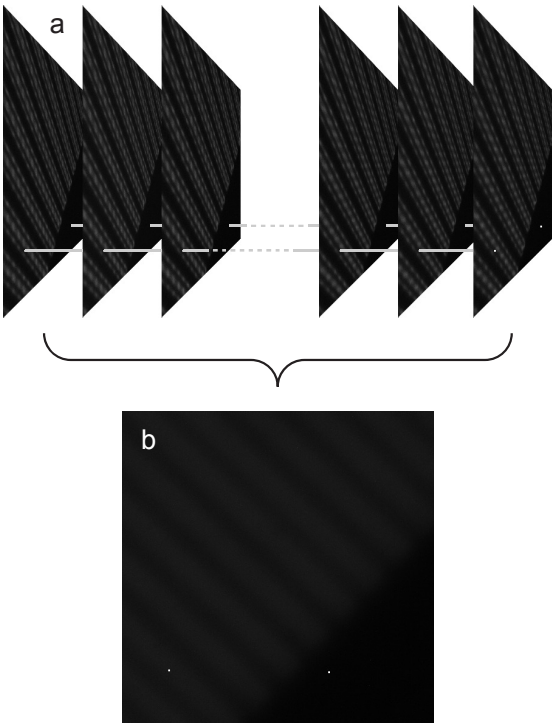

Fig. 2 Illustration of the mean of the whole image stack into the one image. (a) represents the stack of the raw SIM images acquired by the system described in chapter 3. Gray lines correspond to the two hot pixels which appear in all images in the stack. Image (b) is the mean image calculated from the full stack (a) containing two significant hot pixels.

Some kinds of the additional noise (generally white Gaussian noise) can be successfully eliminated by averaging of image dataset with the same content (e.g. the set of astronomy images). In the case of SIM microscopy imaging, each acquired image has a different structure, due to illumination pattern shift, and the averaging is not possible. In order to reduce the presence of the white Gaussian noise, the longer exposure time while acquisition is required. This leads to the boost of dark current influence. Hence, the unwanted hot pixels appearance.

5.1 Hot pixels detection and suppression

Although the hot pixels are randomly distributed within the chip, they are in a fixed position. Therefore, the averaging does not work. The acquiring the dark field image with the same exposure time as the image to be corrected is one possibility to reduce hot pixel in the image. In case, the dark field image is not available, median filtering is commonly used method to remove salt-and-paper noise, which is similar to the hot pixels [18]. However, the median filtering of full SIM image affects the structure of observed sample and the SIM reconstruction does not reach the maximum resolution enhancement. In order to minimize this unwanted effect, the proposed *Hot pixel detection* can be used before the median filtering.

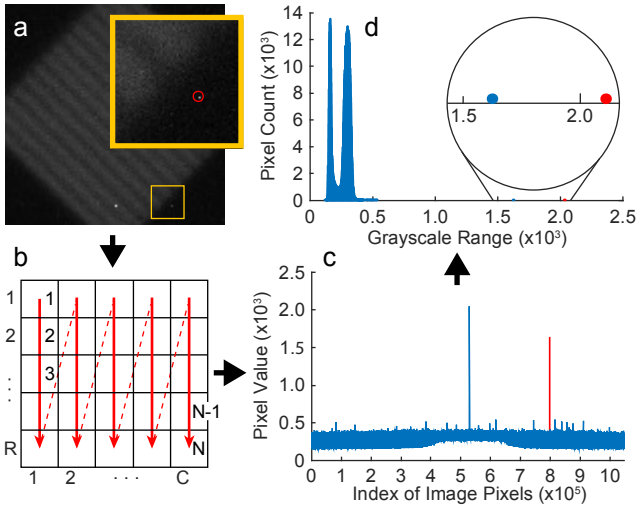

Fig. 3 Representation of an image. (a) is the 2D image of the sum of the whole image stack and contains hot pixels. The yellow rectangle corresponds to the region of interest (ROI) with presence of one hot pixel (signed with red color in (c) and (d)). (b) is a representation of image in a matrix. The 2D image with width C (number of colums) and height R (number of rows) can be represented by 1D vector with total length N = C·R. (c) is the vector representation of (a). Red line corresponds to the hot pixel circled in (a). (d) shows the histogram of (c) (it is equal to the histogram of the (a)). Black arrows mean the flowchart from (a) to (d).

The proposed *hot pixel detection* is based on the threshold estimation using two-term Gaussian model fit on the histogram of the first difference (discrete derivation) of the average image (see Fig. 4). A histogram contains information about light distribution in a digital image. The SIM images have generally two dominant clusters corresponding to the dark background and the usefull signal (see Fig. 4d). Assuming that the SIM image contains the hot pixels, there is a wide gap between these pixels and the useful signal and the assesment of the threshold, which separates the hot pixels, is not complicated. However, there are several hot pixels which value is much lower and the threshold assessment becomes a challenging task.

The main idea of our approach lies in a histogram of the difference (discrete derivation) image, which has a distribution close to the Gaussian distribution instead of the distribution of the average image histogram (see Fig. 4b and d). The Gaussian distribution can be described by the mean value μ, standard deviation σ and amplitude a. In order to calculate this three parameters we used the Gaussian model and the fit function in MATLAB [19], which is defined as:

$$f(x) = \sum_{n=1}^{N} a_n e^{-\frac{(x-\mu_n)^2}{2\sigma_n^2}} \qquad (2)$$

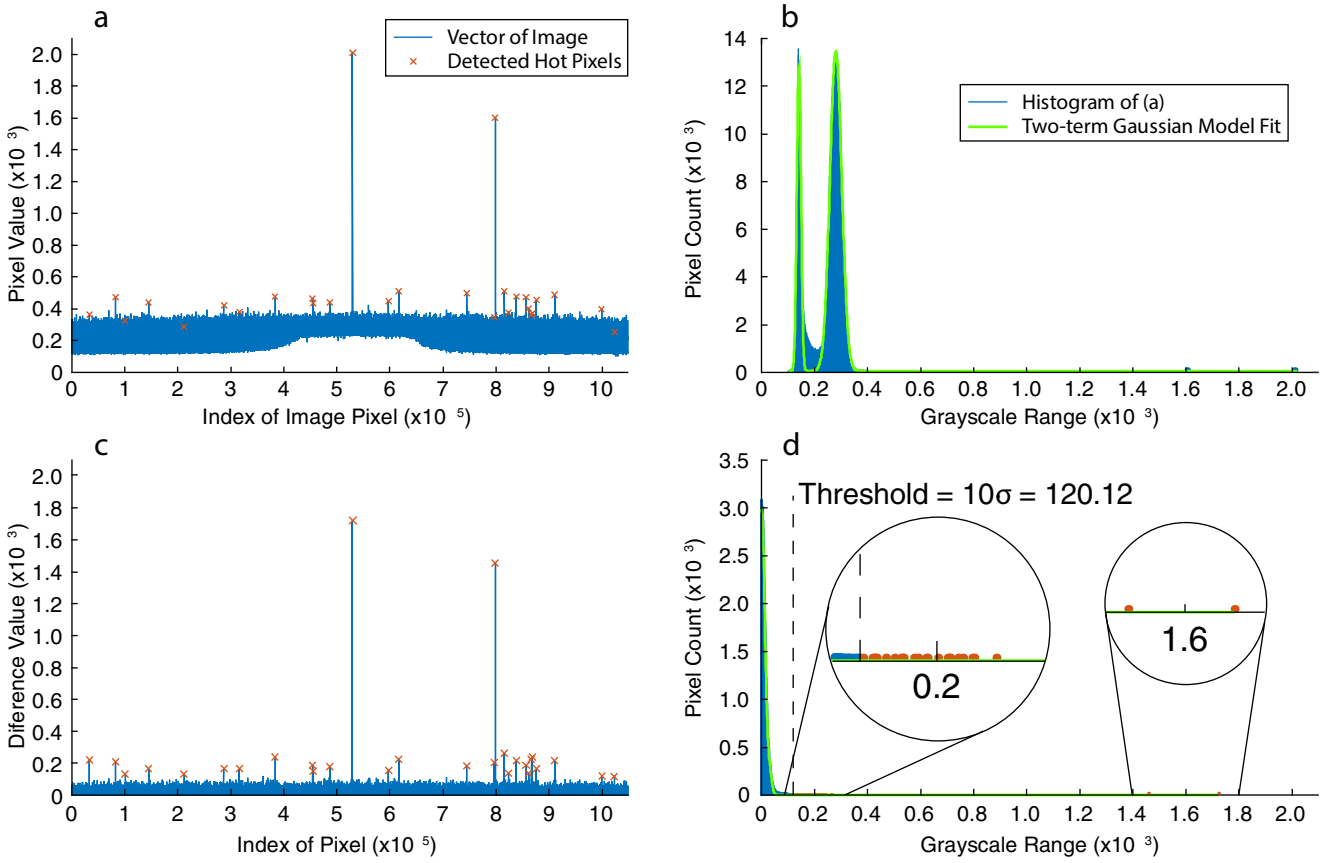

Fig. 4 The principle of the hot pixel detection. (a) shows the 1D representation of the image containing the hot pixels. (b) is the histogram (blue) of image from (a) with the two-term Gaussian model fit (green). (c) shows the first order difference (discrete derivative) of 1D image. (d) corresponds to the histogram (blue) of the first order difference from (c) with two-term Gaussian model fit (green). The red dots represent the detected hot pixel candidates higher than the threshold. These candidates correspond to the red crosses in (a) and (c). The threshold is calculated as six times the full width half maximum (FWHM) of the two-terms Gaussian model fit.

where the n corresponds to the number of Gaussian curves used to fit the data. For more accurate fit, we used two-term Gaussian model ($n = 2$). The total standard deviation σ of two-term Gaussian model with two standard deviations $\sigma_1$and σ_2 is equal to:

$$\sigma = \frac{1}{\sqrt{\frac{1}{\sigma_1^2}+\frac{1}{\sigma_2^2}}}. \tag{3}$$

Further the total mean value μ of this model is then [20]:

$$\mu = \sigma^2\left(\frac{\mu_1}{\sigma_1^2}+\frac{\mu_2}{\sigma_2^2}\right). \tag{4}$$

Assuming that the difference image primarly describes the noise in the original image. The white noise has a Gaussian distribution with zero mean and the information about the sample structure lies within the first and the fourth quartil in the histogram. Therefore, the values lying outside of the fitted function can be considered the hot pixels. The knowledge of the total mean μ and standard deviation σ allows one to calculate the threshold:

$$threshold = \mu + k \cdot \sigma. \tag{6}$$

The k is the constant in range of 5 to 10. Although this approach uses this constant to tune the threshold, the whole hot pixel detection is independent of the dynamic range of the image.

After hot pixel detection, we applied the median filter to each detected pixel in all frames in raw SIM data stack as described in [9].

6. Results and conclusion

Result of the hot pixel detection and suppression is shown in Fig. 5. The image in Fig. 5a is one representative frame of the SIM raw data stack affected by two significant and many weaker hot pixels. The dynamic range of this image is strongly decreased after normalization. By applying our detection and suppression algorithm to all frames in the whole stack, the full dynamic range is utilized after normalization (Fig. 5b).

We have designed a robust method for detection of pixels with significantly higher level than the useful signal in Structured Illumination Microscopy raw image stack. One weakness of this approach is that the algorithm is not completely automatic. Further research is necessary to achieve an automatic operation. However, our method is independent of the dynamic range of input image. Further,

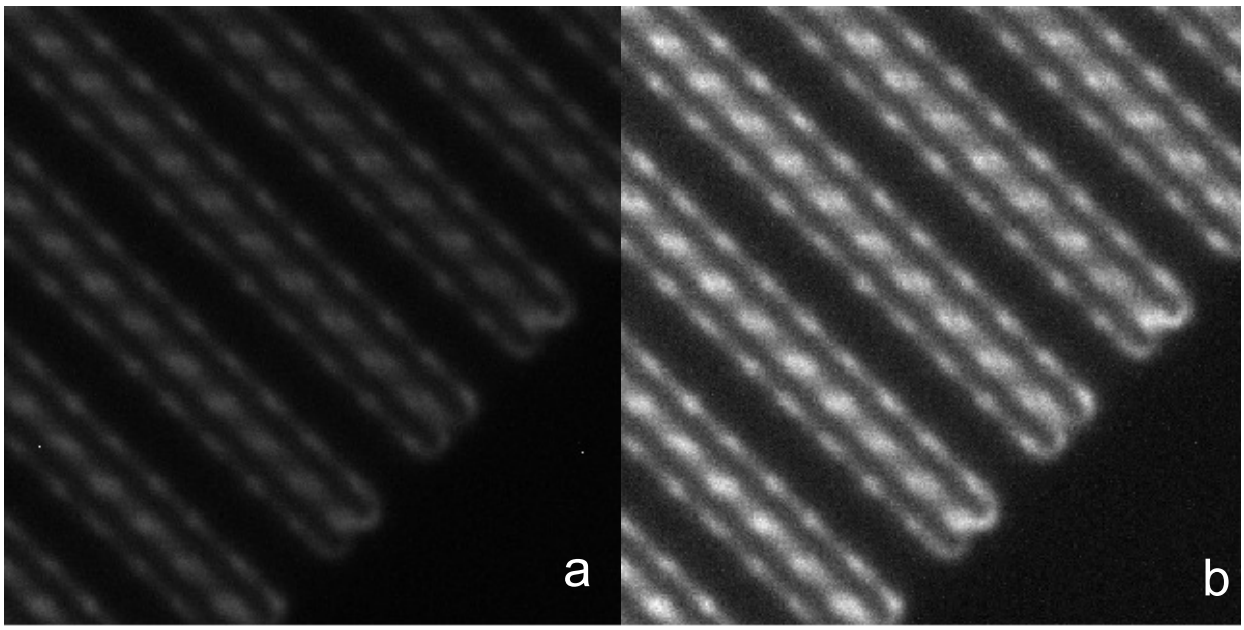

Fig. 5 The result of hot pixel detection and suppression. Both images represent the ROI of sum of whole stack normalized according the highest value in the image. Image (a) contains two significant hot pixels, which dramatically decrease the dynamic range. Image (b) shows the result of our algorithm.

our detection approach works well in case that there is no hot pixel in the image (i.e. no false detection). A difference image reveals the lower hot pixels in the background which may be considered a useful signal after simple image thresholding. This input image preprocessing could be an essential part of SIM reconstruction for data without a calibration.

Acknowledgements

Research described in the paper was supervised by Prof. Miloš Klíma and Dr. Karel Fliegel, Faculty of Electrical Engineering, Czech Technical University in Prague. This research was supported by the Czech Technical University student grant (SGS16/167/OHK3/2T/13). The author would like to thank Guy Hagen for providing the structured illumination microscopy data and Tomáš Lukeš for his insightful comments.

References

[1] GUSTAFSSON, M. G. L., "Surpassing the lateral resolution limit by a factor of two using structured illumination microscopy," *J. Microsc.*, vol. 198, no. 2, pp. 82–87, 2000.

[2] RUST, M. J., BATES, M., and ZHUANG, X., "Stochastic optical reconstruction microscopy (STORM) provides sub-diffraction-limit image resolution," *Nat. Methods*, vol. 3, no. 10, pp. 793–795, 2006.

[3] DERTINGER, T., COLYER, R., IYER, G., WEISS, S., and ENDERLEIN, J., "Fast, background-free, 3D super-resolution optical fluctuation imaging (SOFI)," *Proc. Natl. Acad. Sci. U. S. A.*, vol. 106, no. 52, pp. 22287–92, 2009.

[4] GEISSBUEHLER, S., BOCCHIO, N. L., DELLAGIACOMA, C., BERCLAZ, C., LEUTENEGGER, M., and LASSER, T., "Mapping molecular statistics with balanced super-resolution optical fluctuation imaging (bSOFI)," *Opt. Nanoscopy*, vol. 1, no. 1, p. 4, 2012.

[5] BETZIG, E. *et al.*, "Imaging intracellular fluorescent proteins at nanometer resolution.," *Science*, vol. 313, no. 5793, pp. 1642–5, 2006.

[6] HELL, S. W. and WICHMANN, J., "Breaking the Diffraction Resolution Limit By Stimulated-Emission - Stimulated-Emission-Depletion Fluorescence Microscopy," *Opt. Lett.*, vol. 19, no. 11, pp. 780–782, 1994.

[7] LUKEŠ, T. *et al.*, "Three-dimensional super-resolution structured illumination microscopy with maximum a posteriori probability image estimation.," *Opt. Express*, vol. 22, no. 24, pp. 29805–29817, 2014.

[8] KŘÍŽEK, P., LUKEŠ, T., OVESNÝ, M., FLIEGEL, K., and HAGEN, G. M., "SIMToolbox: A MATLAB toolbox for structured illumination fluorescence microscopy," *Bioinformatics*, vol. 32, no. 2, pp. 318–320, 2015.

[9] BAILEY, D. and JIMMY, J. S., "FPGA Based Multi-shell Filter for Hot Pixel Removal within Colour Filter Array Demosaicing," in *International Conference on Image and Vision Computing New Zealand*, 2016, p. 6.

[10] CAO, Y. and ZHANG, X., "An on-chip hot pixel identification and correction approach in CMOS imagers," *SoC Des. Conf. (ISOCC), 2011 ...*, pp. 408–411, 2011.

[11] CHAPMAN, G. H., THOMAS, R., THOMAS, R., KOREN, I., and KOREN, Z., "Improved correction for hot pixels in digital imagers," *Proc. - IEEE Int. Symp. Defect Fault Toler. VLSI Syst.*, pp. 116–121, 2014.

[12] CAO, Y., TANG, F., BERMAK, A., and LE, T. M., "A smart CMOS image sensor with on-chip hot pixel correcting readout circuit for biomedical applications," *Proc. - 5th*

IEEE Int. Symp. Electron. Des. Test Appl. DELTA 2010, pp. 103–107, 2010.

[13] KŘÍŽEK, P., RAŠKA, I., and HAGEN, G. M., "Flexible structured illumination microscope with a programmable illumination array," *Opt. Express*, vol. 20, no. 22, p. 24585, 2012.

[14] LUKEŠ, T. and HAGEN, G., "Comparison of image reconstruction methods for structured illumination microscopy," *Proc. SPIE 9129*, vol. 9129, no. June, pp. 1–13, 2014.

[15] HOWELL, S. B., *Handbook of CCD Astronomy*, 2nd ed. New York: Cambridge university press, 2006.

[16] WILKINSON, M. H. F. and SCHUT, F., *Digital Image Analysis of Microbes: Imaging, Morphometry, Fluorometry and Motility Techniques and Applications*, 1st ed. New York, USA: John Wiley & Sons, Inc. New York, NY, USA ©1998, 1998.

[17] GULLIXSON, C., "Astronomical CCD observing and reduction techniques," in *Astronomical Society of the Pacific*, 1992, p. 345.

[18] PCO IMAGING, "Warm/Hot pixel," 2010. [Online]. Available: https://www.pco.de/fileadmin/user_upload/db/download/kb_hot_pixel_20100813.pdf. [Accessed: 13-Aug-2010].

[19] THE MATHWORKS INC., "MATLAB and Statistics Toolbox Release 2015b." Natick, Massachusetts, United States, 2015.

[20] BROMILEY, P. A, "Products and Convolutions of Gaussian Distributions," *Biomed. Eng. (NY).*, vol. M, no. 2003, 2003.

Jakub POSPÍŠIL was born in Jindřichův Hradec, Czech Republic in 1990. In 2013 he received his bachelor diploma from Communications, Multimedia, and Electronics program at Faculty of Electrical Engineering (FEE), Czech Technical University (CTU) in Prague. He graduated form of the same master's degree program in 2015. He is currently a PhD student in Multimedia Technology Group (MMTG) with department of Radioelectronics at FEE in CTU in Prague. His research interests include the super-resolution microscopy, especially the Structured Illumination Microscopy (SIM).

Supplementary

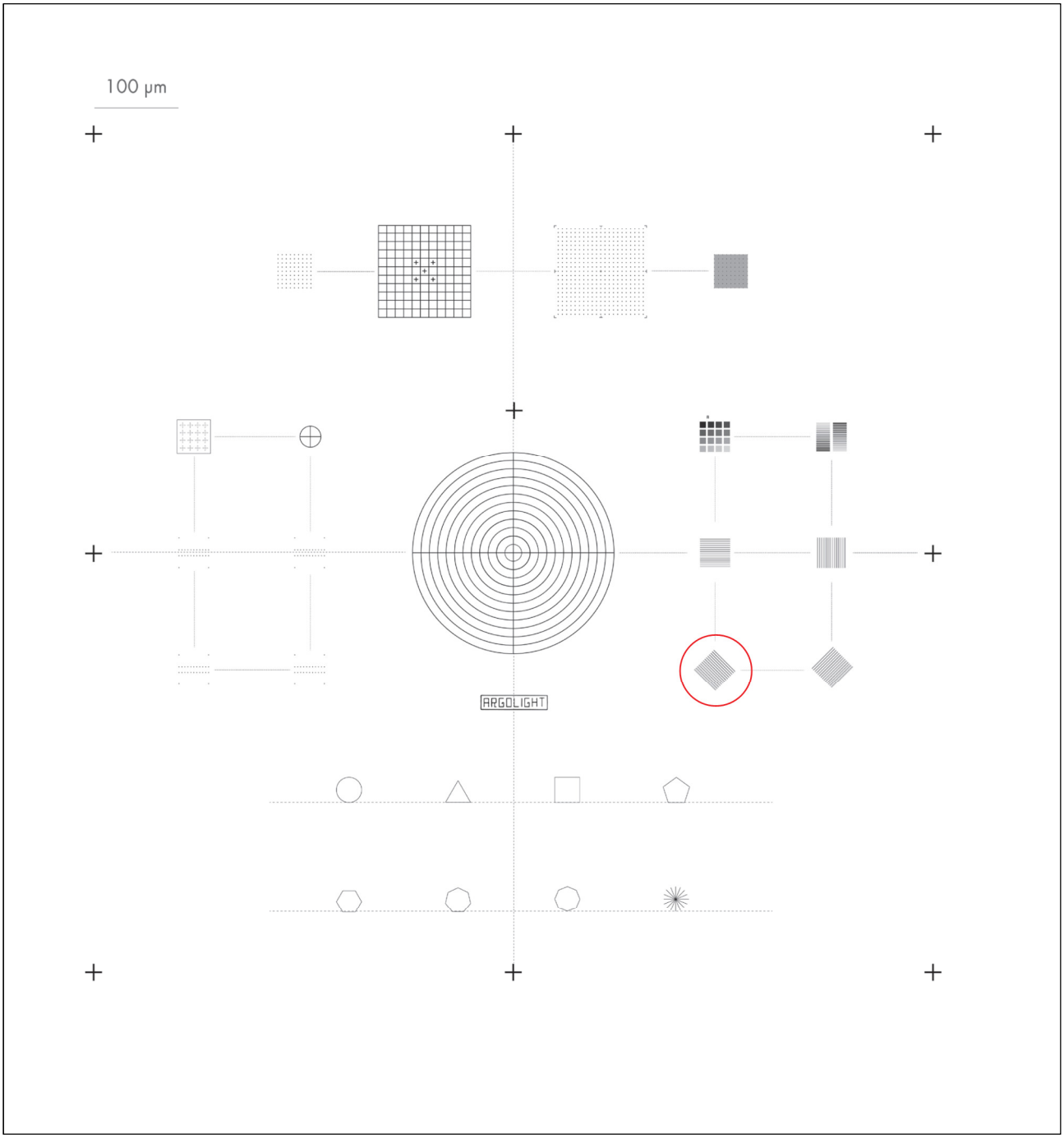

Fig. 6 Patterns overview. Matrix of rings, grid, 2D matrix of rings, matrix of rings on a background, matrix of crosses, meridians of a sphere, repositioning crosses, 4x4 intensity, 2x16 intensity, 3D crossing stairs, target, logo, geometrical figures and gradually spaced lines - 36 µm long lines which spacing gradually increases, from 80 to 340 nm. Red circuit highlights ROI used in our experiment.